Geophysical Research Letters

RESEARCH LETTER
10.1002/2018GL077477

Key Points:
- We identify a powerful, short-lived thermal event in the vicinity of Marduk Fluctus in *Galileo* NIMS Io data
- The temporal evolution of this event is consistent with an explosion, with rapid cooling suggesting the generation of small clasts
- Similar events imaged from spacecraft will constrain lava eruption temperature if data are obtained simultaneously at multiple wavelengths

Correspondence to:
A. G. Davies,
ashley.davies@jpl.nasa.gov

Citation:
Davies, A. G., Davies, R. L., Veeder, G. J., de Kleer, K., de Pater, I., Matson, D. L., et al. (2018). Discovery of a powerful, transient, explosive thermal event at Marduk Fluctus, Io, in *Galileo* NIMS data. *Geophysical Research Letters*, *45*, 2926–2933. https://doi.org/10.1002/2018GL077477

Received 6 FEB 2018
Accepted 9 MAR 2018
Accepted article online 14 MAR 2018
Published online 6 APR 2018

©2018. American Geophysical Union. All Rights Reserved.

Discovery of a Powerful, Transient, Explosive Thermal Event at Marduk Fluctus, Io, in *Galileo* NIMS Data

A. G. Davies[1], R. L. Davies[2], G. J. Veeder[3], K. de Kleer[4], I. de Pater[5], D. L. Matson[3], T. V. Johnson[1], and L. Wilson[6]

[1]Jet Propulsion Laboratory, California Institute of Technology, Pasadena, CA, USA, [2]Oxted School, Oxted, Surrey, UK, [3]Bear Fight Institute, Winthrop, WA, USA, [4]California Institute of Technology, Pasadena, CA, USA, [5]Department of Astronomy, University of California Berkeley, Berkeley, CA, USA, [6]Lancaster Environment Centre, Lancaster University, Lancaster, Lancashire, UK

Abstract Analysis of *Galileo* Near-Infrared Mapping Spectrometer observations of Marduk Fluctus, a volcano on the Jovian moon Io, reveals a style of volcanic activity not previously seen there—a powerful thermal event lasting only a few minutes in 1996. The thermal emission rapidly fades, suggesting extremely rapid cooling of small clasts. The duration and evolution of the explosive eruption are akin to what might be expected from a strombolian or vulcanian explosion. The presence of such events provides an additional volcanic process that can be imaged by future missions with the intent of determining lava composition from eruption temperature, an important constraint on the internal composition of Io. These data promise to be of particular use in understanding the mechanics of explosive volcanic processes on Io.

Plain Language Summary A very brief but powerful volcanic explosion has been identified on Io, the highly volcanic moon of Jupiter, in data collected by the imaging spectrometer on NASA's *Galileo* spacecraft in 1996. This event is likely driven by a build-up of gas, resulting in explosive activity, perhaps similar to that regularly seen at Stromboli volcano on Earth. The huge explosion in the Marduk region of Io likely created a myriad of tiny lava fragments that cooled very rapidly, which explains the speed at which the resulting thermal anomaly decayed back to background, preexplosion levels. Similar events, ideally observed from close to Io by instruments on some future mission to this volcanic wonder, could help answer one of the biggest questions remaining in the wake of the *Galileo* mission, that of the dominant composition of Io's highly voluminous lavas. This determination would be accomplished by measuring the temperature of the lava as it erupts. Such a measurement would strongly constrain Io's interior composition and current state, which is important for understanding the evolution of the large Galilean satellites (including the ice-covered Europa).

1. Introduction

The highly volcanic Jovian moon Io exhibits many different modes of eruption and emplacement of lava onto the surface (e.g., Davies, 2007; Davies et al., 2010). Observed and implied styles of eruption are similar to those seen on terrestrial basalt volcanoes (active, overturning lava lakes; pahoehoe-like insulated flows; open-channel flows; lava fountaining) (Davies, 2007). Ionian volcanic activity is typically on much larger areal and volumetric scales than contemporary terrestrial eruptions. Observations of thermal emission from Io's erupting volcanoes can be used to constrain the composition of Io's lavas (Davies et al., 2001, 2017; McEwen et al., 1998). This is important as the composition of the erupting lava reflects the degree of melting in the upper mantle (Keszthelyi et al., 2007), which is a direct consequence of the depth and magnitude of tidal heating due to the Laplace resonance. However, only eruption styles that reveal relatively large areas at temperatures very close to the eruption temperature are suitable for this purpose. The best targets for instruments on spacecraft flying close to Io include targets such as the bases of lava fountains (Keszthelyi et al., 2001) and the lava stream within a lava tube as viewed through a skylight (Davies et al., 2016). *Galileo* Near-Infrared Mapping Spectrometer (NIMS) data obtained in 1996, but only recently examined in detail, reveal another process that might be suitable for determining eruption temperatures: transient, short-wavelength infrared thermal events reminiscent of a large explosion on Io's surface. Such an event was observed at or near to the active volcano Marduk Fluctus.

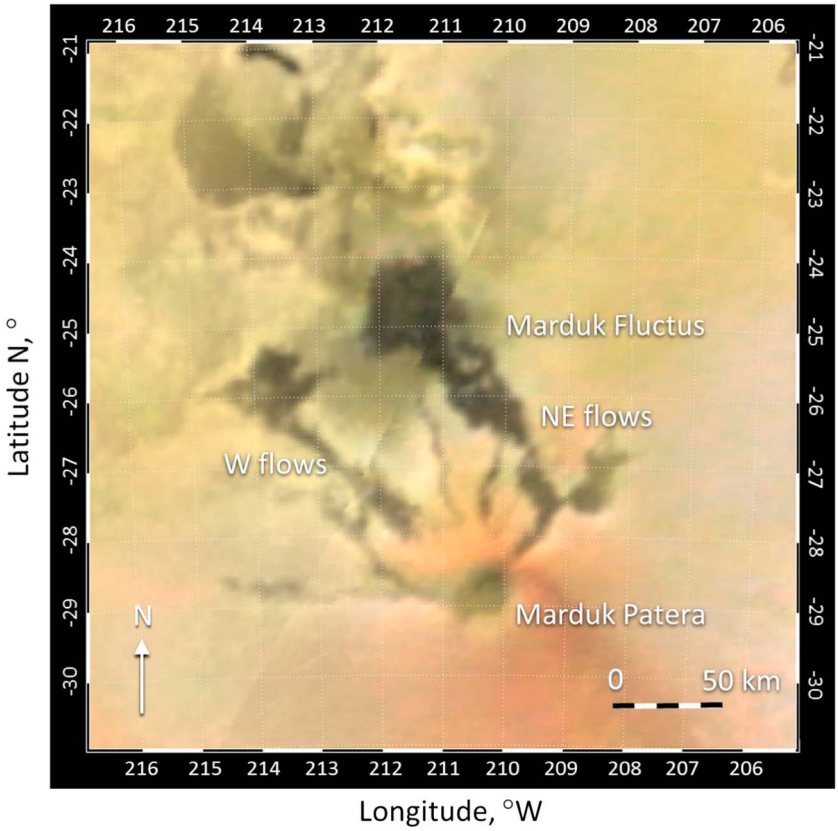

Figure 1. The Marduk Fluctus volcanic complex as seen by the *Galileo* Solid-State Imaging experiment. Flows originate in a patera (a caldera-like volcanic depression) in the south of the image and flow northward. The reddish deposit is rich in sulfur. Image derived from the Io global mosaic of Becker and Geissler (2005). See also Williams et al. (2011).

2. Observations

2.1. *Galileo* NIMS and Observations of Io

The *Galileo* NIMS instrument (Carlson et al., 1992) was well suited to measuring the thermal emission from Io's volcanoes, as the 0.7 to 5.2-μm wavelength range meant that NIMS was sensitive to surface temperatures from ~220 to >1000 K (Davies et al., 2010). The acquisition and processing of the high-precision NIMS radiance data are described in detail by Davies (2007). NIMS obtained 190 Io observations between 1996 and 2001. Twenty-seven observations of Io were obtained during *Galileo* orbit E4 between 17 and 19 December 1996. Many of these observations were designed to look for short-term variations in volcanic thermal emission. Six observations of Io obtained on 18 and 19 December 1996 covered much of the trailing hemisphere of Io (180°W to 360°W), including the location of Marduk Fluctus (209.9°W, 28.4°S), a powerful and persistent volcano. Planetary Data System NIMS raw radiance "tube" products were used to measure radiance, and "cube" products, which have improved navigation, to identify hot spot location (e.g., Davies et al., 2012).

2.1.1. Marduk Fluctus

Marduk Fluctus (Figure 1) has an extensive flow field identified early in the *Galileo* mission at Jupiter as a thermal source by both the *Galileo* Solid-State Imaging experiment (SSI) (observation G1ISIOECLI02) (Belton et al., 1996; McEwen et al., 1997) and NIMS (Lopes-Gautier et al., 1997). The Marduk region was identified as a plume source in 1979 *Voyager* data (Strom et al., 1981), and SSI observed changes between the first two *Galileo* orbits in 1996. Marduk Fluctus has been identified as a thermal source in multiple NIMS observations (Figure 2) and ground-based telescope data (e.g., de Pater, Davies, McGregor, et al., 2014). SSI data show Marduk Fluctus as consisting of a series of at least six lava flows emanating from a patera and likely flowing downslope, consistent with the flows spreading laterally into a broad fan as the gradient decreases. Around

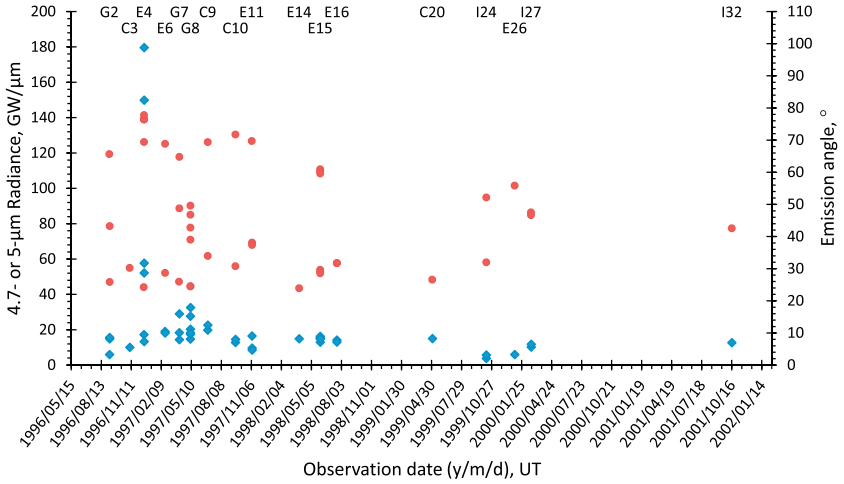

Figure 2. The values 4.7 or 5-μm radiances (blue diamonds) are corrected for emission angle (angles shown as red circles) from Near-Infrared Mapping Spectrometer observations that include Marduk Fluctus. *Galileo* orbit designations are also shown. The orbit E4 radiance values are unmatched, even in other observations taken at high emission angles.

the vent is a reddish plume deposit, likely rich in short-chain sulfur allotropes (Geissler et al., 1999). The presence of these short-lived deposits is an indication of ongoing high-temperature (silicate) volcanic activity. The area is marked by what are presumably older flows which have cooled to the point where sulfur and SO_2 condense on the surface, yielding higher albedos than the active flows. The area of the young, black lava flows is ≈3,600 km^2 (Veeder et al., 2009, 2012).

2.1.2. Marduk Fluctus E4 NIMS Observations

Between 1996 and 2001 NIMS obtained 44 usable Io observations that included Marduk Fluctus (Figure 2). Six E4 observations (see Table 1) were obtained where thermal emission was detected from Marduk Fluctus on 18 and 19 December 1996. Marduk Fluctus was in darkness in the five latter observations, which were made on the outbound portion of *Galileo*'s orbit. At a range of 319,480 km, spatial resolution was 160 km/pixel for the first, day-lit observation (e4i007tr), which had an emission angle of 24.3°. NIMS observation e4i007tr measured radiance at 96 wavelengths across the full NIMS range. The five usable nighttime observations were obtained at ranges from 752,083 to 905,805 km, yielding spatial resolutions from 376 to 453 km/pixel, and at emission angles of 69.4° to 77.8°. More important than spatial resolution in this case is spectral resolution. NIMS obtained data at 10 to 12 wavelengths spread evenly across the NIMS wavelength range, allowing constraint of emitting areas and temperatures. This spectral resolution is somewhat problematic as radiation-induced spikes in the NIMS data are often detectable by their deviation from other data close by in the spectrum. Also, problems with NIMS detectors 1 and 2 (<1 μm) render these data unreliable. Where data have been fitted with the black-body thermal emission model (see below), an effort was made to ensure that most data fall on or below the resulting curve to maximize the integrated thermal emission (Davies, 2003). The uncertainty of the despiking and the inherent scatter within the e4i006tr and e4i025tr data reduces confidence in the temperature derivations such that a strong constraint on lava eruption temperature is not possible. However, the present analysis is based on the comparison of the overall shape of the thermal emission spectra and relative intensity of thermal emission from observation to observation, tasks for which the data are well suited. There was no clear detection of Marduk Fluctus in another nine observations obtained during E4 at high emission angles and low spatial resolution, especially where data were so heavily impacted by radiation as to render them unusable. Usable NIMS E4 Marduk Fluctus nighttime data are shown in Figure 3a.

3. Methods

Near-Infrared Mapping Spectrometer radiance data are processed by adding radiances from adjacent pixels to account for the NIMS point-spread function (e.g., Davies, 2007). Obvious radiation-induced spikes are removed. An emission angle correction is applied. If the thermal emission source was essentially a flat

Table 1
Characteristics of NIMS E4 Observations Including Marduk Fluctus and Boundary Two-Temperature, Two-Area Model Fits

Observation	Observation id	Date, time	No. of NIMS λ	Range km	Emission angle °	Temp 1 K	Area 1 km^2	Temp 2 K	Area 2 km^2	Power area 1 GW	Power area 2 GW	Total power[a] GW
e4i007tr (1)	E4INHRSPEC01[b]	18/12/1996 21:29	96	319,480	24.3	284	3,600	—	—	1328	—	1,328
e4i006tr (1)	E4INCOOLCV02C	10/12/1996 13:40	10	752,083	69.4	1,400	0.2	440	100	44	213	256
e4i017tr (1)	E4INWARMCV03A	19/12/1996 15:56	10	880,418	76.4	1,144	10.8	496	201	1,047	689	1,735
e4i017tr (2)	E4INWARMCV03A	19/12/1996 15:56	10	880,418	76.4	1,144	2.52	496	46.9	245	161	406
e4i017tr (3)[c]	E4INWARMCV03A	19/12/1996 15:56	10	880,418	76.4	1,085	2.71	—	—	212	—	212
e4i018tr (1)	E4INWARMCV03B	19/12/1996 15:57	10	881,752	76.5	1,332	4.2	567	142	741	834	1,575
e4i018tr (2)	E4INWARMCV03B	19/12/1996 15:57	10	881,752	76.5	1,332	0.98	567	33	175	193	368
e4i018tr (3)	E4INWARMCV03B	19/12/1996 15:57	10	881,752	76.5	1,368	0.49	899	2.22	98	82	180
e4i019tr (1)	E4INWARMCV03C	19/12/1996 15:58	10	882,869	76.5	1,722	0.5	714	15.0	238	221	459
e4i019tr (2)	E4INWARMCV03C	19/12/1996 15:58	10	882,869	76.5	1,722	0.12	714	3.5	60	52	112
e4i019tr (3)[c]	E4INWARMCV03C	19/12/1996 15:58	10	882,869	76.5	1,800	0.05	—	—	29	—	29
e4i025tr (1)	E4INWARMCV04A	19/12/1996 16:21	10	905,805	77.8	830	1.4	290	1×10^4	38	4,010	4,048
e4i025tr (2)	E4INWARMCV04A	19/12/1996 16:21	10	905,805	77.8	830	0.29	290	2133	8	847	855

Note. (1) Model fits to data corrected for emission angle. (2) Model fits to "explosion" data not corrected for emission angle. (3) Model fits to "explosion" data not corrected for emission angle, having subtracted emission angle corrected e4i006tr data.
[a]An emissivity e of 1 is used. [b]e4i007tr temperature and area derived from 4.999-μm radiance of 17.26 GW/μm from an area of 3,600 km^2 (Veeder et al., 2012). [c]Data best fitted with single component.

plate (a broad lava flow or a lava lake surface), and thermal emission was Lambertian, then dividing the radiances by the cosine of the emission angle would be appropriate to determine the actual emitting areas and thermal emission. However, as lava flows are not two-dimensional and thermal emission can be detected at emission angles ⩾70°, then the cosine correction may exaggerate the power and area of the thermal source. Additionally, if the thermal source was above the surface—a lava fountain, for example, or clasts from an explosion—then a cosine correction should not be applied. The suitability of applying the cosine correction in this particular case is discussed below. The NIMS data are fitted with a two-temperature, two-area ("2-T, 2-A") model (e.g., Davies et al., 1997, 2001). The model minimizes the residuals between the data and the model output. The resulting relatively small, hot area is the sum of the hot vent (if present), young lava surfaces including new lava breakouts, lava fountains, incandescent open channel flows, and areas within a lava lake or pond where the crust is being disrupted. The lower temperature component, a much larger area in these cases, corresponds to the cooling and insulating crust that forms on lava flows and lava lakes.

4. Results

The NIMS data are mostly well constrained by the 2-T, 2-A model. Figure 3 shows the evolution of the thermal event. Data are processed in three ways to account for uncertainty in the vertical extent of the lava (and hence the appropriate emission angle correction to use), and all three processed data sets are fitted with the 2T, 2A model (Table 1). First, all data are corrected for emission angle (Figure 3a). This represents the upper limit of thermal emission. Second, the data showing the thermal spike (e4i017tr, e4i018tr, and e4i019tr) are left uncorrected for emission angle (Figure 3b). Third, the thermal spike data are not corrected for emission angle and have the emission angle corrected e4i007tr "pre-event" spectrum subtracted. This isolates the spike's thermal component from the background and is the lower boundary of the event's thermal emission. The resulting spectra are shown in Figure 3b.

Considering data that have been corrected for emission angle, at some time in the 136 min between observations e4i006tr and e4i017tr thermal emission increased by more than an order of magnitude at all wavelengths. In the next 2 min and 2 s, between e4i017tr and e4i019tr thermal emission decreased rapidly, mostly at wavelengths between 3.5 and 5.2 μm. There was a shortening of the peak of thermal emission from 2.7 μm for e4i017tr, suggesting an effective brightness temperature T_{eff} of 1035 K, to 2.4 μm for e4i018tr (T_{eff} = 1,207 K), to 1.8 μm for e4i019tr (T_{eff} = 1,610 K). As 2-T, 2-A fits may underestimate the temperature of the hottest areas present, the actual eruption temperature may be well in excess of 1,600 K, which would suggest an ultramafic lava composition. Over the same time interval, the hot component area tracks the rise and fall of thermal emission starting at a fraction of a km^2, rising to an area of 11 km^2, then rapidly decaying to an area of less than 1 km^2 again. After another 23 min, thermal emission across short NIMS wavelengths has dropped to below the pre-event background level at these wavelengths.

However, at wavelengths longer than 4 μm, a slope develops in the data, suggesting an additional larger, cool component is present, one that was not present in the e4i006tr observation. The measured spectral radiance

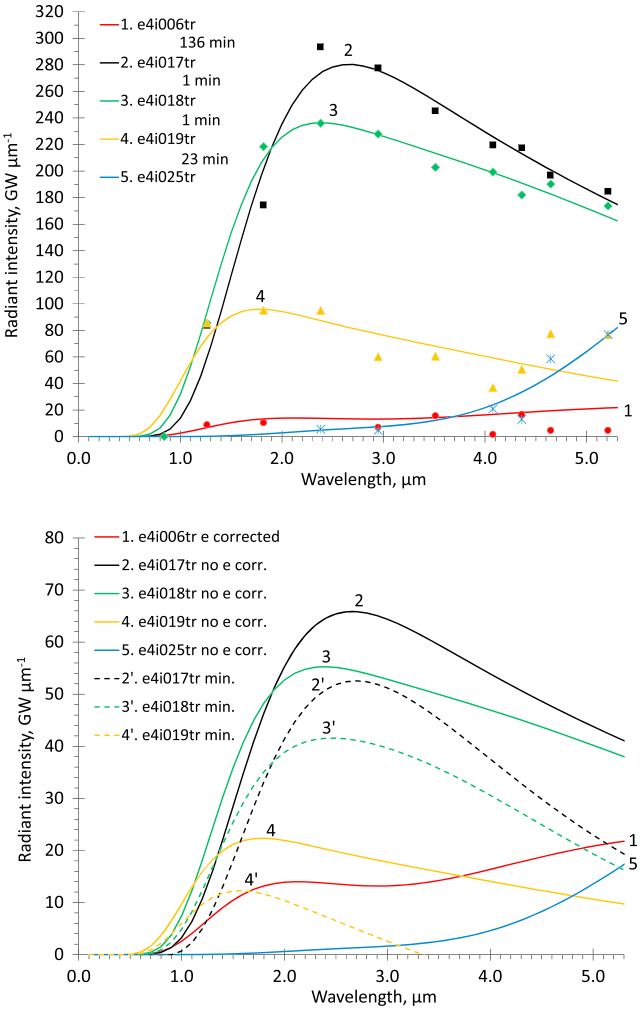

Figure 3. (a) Radiances from Marduk Fluctus (symbols) and thermal emission model spectra (solid lines) synthesized from the best two-temperature, two-area fits to the data using the temperatures and areas in Table 1. The numbers refer to the order in which the observations were obtained. Data are corrected for emission angle. The intervals between observations are also shown. (b) Radiances uncorrected for emission angle *e* (solid lines). The lower boundary of thermal emission is obtained by subtracting the pre-event *e*-corrected e4i006tr radiance (1) from the uncorrected radiance spectra from the "explosion" observations (e4i017tr, e4i018tr, and e4i019tr, denoted by 2′, 3′, and 4′).

demonstrates a shift in the peak in thermal emission to longer wavelengths (suggesting a lower temperature) from e4i019tr to e4i025tr. The e4i019tr data suggest a rapidly dwindling hot area and a new, large, cool area that is still detectable in the e4i025tr data. We note that the model fits to the e4i019tr and e4i025tr data are poorly constrained because of scatter of the sparse data. It is apparent that some of the data are impacted by data dropout and noise. In line with previous practices (Davies, 2003), model fits are to the upper boundary of the remaining data. Doing so with the e4i025tr data yields a cool area of 10,000 km^2 at 290 K. This might be a cool plume or blanket of small pyroclastics resulting from the explosion. We can only speculate as to what this may represent. The lack of a 200-km diameter low-albedo (silicate-rich) deposit in subsequent *Galileo* imagery suggests that this deposit either does not exist or was buried under later, higher-albedo, sulfur-rich plume fallout. Fitting by weighting the lower data points between 3.5 and 5.2 µm yields a smaller cool component area covering 190 km^2 at 395 K. In any event, the low level of thermal emission in e4i025tr shows rapid cooling, consistent with the explosion hypothesis discussed below.

5. Discussion

The radiance from this event, with such rapid waxing and waning in radiance at all wavelengths and with such large variations in intensity, changes more rapidly than has been previously seen on Io (Blaney et al., 1995; Davies, 1996; Sinton et al., 1983). We can speculate as to what physical process generates this thermal signal evolution. The increase in short wavelength thermal emission can be explained by the exposure of incandescent lava erupting at temperatures well in excess of 1,000 K. This could be caused by a new outbreak of lava, a lava fountain issuing from a fissure, fountaining in a lava lake, or the rapid overturning and replacement of crust in a lava lake; all of these processes generate strong increases in short wavelength thermal emission (Davies et al., 2010). However, the E4 thermal spike is unique with the thermal emission returning to the pre-event level very quickly (a few minutes). Newly exposed incandescent lava initially cools very rapidly, but the rate of cooling decreases as temperature decreases. On Io, basalt cools from 1,475 to 1,100 K in about a minute and to 1,020 K in 2 min, but it takes another 1.6 hr to cool to 700 K and another 32 hr to cool to 500 K (Davies, 1996). The thermal signal in the E4 data reached the pre-event background level in no more than 23 min (the time between e4i017tr and e4i025tr). A replaced crust on a lava lake does not cool fast enough to explain the data. The eruption of a new lava flow would have to be very brief (less than a few minutes) and still cover multiple km^2 before abruptly stopping and would still not cool fast enough to depress the thermal emission to the observed postevent level.

The E4 nighttime observations were obtained at high emission angles (69.4° to 77.8°), so thermal emission may be partially blocked by topography. However, observation e4i007tr was obtained at a low emission angle (24.3°), showing that, at least in the east-west direction, topographic shielding is not taking place (e.g., de Kleer & de Pater, 2017; Radebaugh et al., 2002). The "background" level of thermal emission does decrease slightly at short wavelengths after the thermal event, but the emission angle difference is $<2°$ from that of the peak of the eruption and so topographic control is unlikely. The thermal emission from the Marduk Fluctus lavas, likely from lava flows dominated by a relatively cool insulating crust, is visible at high emission angles and is therefore not shielded by topography. Likewise, if the thermal emission from Marduk Fluctus is emanating from a lava lake, then the lava lake surface is not topographically shielded either. Of the ≈40 other

NIMS observations of this area (Figure 2), the thermal emission at 5 μm is constant at about 15 ± 6 GW/μm over a wide range of emission angles (excluding the E4 thermal event data). The E4 data cannot be explained simply by the emplacement of a new lava flow or the quiescent replacement of the crust in a lava lake.

The E4 event had to be caused by a different style of activity. We propose that this event was a short-duration eruption event—such as a strombolian or vulcanian explosion. It is unlike most terrestrial strombolian activity in as much as this appears to be a single event, and terrestrial strombolian eruptions are episodic. However, poor temporal resolution over much of the duration of the *Galileo* mission may have prevented other similar events from being detected; alternatively, other such events simply have not yet been identified in the NIMS data.

Strombolian events are driven by the abrupt release of gas that has accumulated within the ascending magma when the pressure becomes too great to be contained. On Io, as magma ascends through the lithosphere, it can thermally interact with interbedded layers of pyroclastic material, lava flows, and plume deposits rich in SO_2 and sulfur and may therefore add volatiles to any primary volatiles already present in the magma (Leone et al., 2011).

Such explosions have been observed in the phonolite lava lake of Erebus volcano, Ross Island, Antarctica (e.g., Gerst et al., 2013). The contents of the lava lake, which in December 2005 was 38 m across (Davies et al., 2008), were entirely evacuated and disrupted into fragments. These fragments, ranging in size typically from mm to in excess of 1 m in diameter, are ejected at velocities often exceeding 50 m/s (Gerst et al., 2013). In 2005–2006, bombs were distributed as far as 600 m from the lava lake (Gerst et al., 2008), and explosions occurred every 6 to 9 hr. After such an explosion, the lava lake quickly refilled and within a few minutes (as witnessed by the lead author), appeared as it did before the explosion.

An explosion in a lava lake can also be caused by the fall of material from the crater wall into the lava lake. This has been observed repeatedly at the lava lake that began forming in 2008 in Halema'uma'u, Kilauea volcano, Hawai'i. The lava lake enlarges through failure of the undermined walls of the pit in which it resides. Rockfall into the lake apparently triggers the abrupt release of volatiles in lava close to the surface, possibly by runaway decompressive vesiculation, leading to an explosion (Orr et al., 2013). The explosion, possibly exacerbated by the formation of a rebound-splash Worthington jet (Orr et al., 2013), and the generation of an ash cloud that includes juvenile tephra, is followed by powerful roiling of the lava until equilibrium is restored. Eventually, the lava lake surface temperature distribution returns to preeruption levels.

On Io, such a gas-driven explosion would be enhanced by the environment. The lack of a substantial atmosphere allows unrestrained expansion of the gas, increasing the fragmentation of the lava and increasing ejection velocity over a similar eruption on Earth. The lower gravity on Io increases the range (Wilson & Head, 1983).

Phreatomagmatic activity can also cause explosions on basaltic volcanoes. A rootless explosion may be caused by the thermal mobilization of surface ices underneath a thick lava flow. Such an explosion was observed during the Eyjafjallajökull, Iceland eruption in 2010 (A. Hoskuldsson, personal communication, 2010). In 1924 and 2008, ground water interacting with hot rock caused ash-rich explosions on Kilauea volcano, Hawai'i (e.g., Houghton et al., 2011; Mastin, 1997).

Rather than being strombolian, the explosion may be vulcanian in nature. Although vulcanian eruptions are generally associated with more viscous lava than basalt, the collection of gas-rich lava under the cooled crust of a lava lake or lava flow could build up pressure to the point that an explosion occurs.

An explosion of some kind best explains the *Galileo* orbit E4 NIMS Marduk Fluctus data. A powerful explosion would generate clasts that, if very small, would cool rapidly. On Io, a basalt clast of radius 1 mm would cool from 1,480 to 700 K in less than a minute (Keszthelyi et al., 2007) and would cool to 520 K in 2 min and to 290 K in just over 12 min. The explosive generation of small clasts, initially erupted at a liquidus temperature at or above 1,400 K, would generate the observed thermal spike and subsequent rapid thermal decay as the clasts were widely dispersed and rapidly cooled. Similar small clasts formed during lava fountaining events that took place on the early Moon (Wilson & Head, 1981, 1983).

The emitted power P from each clast = $4\pi R^2 \sigma T^4$, where R is the clast radius, T is absolute clast temperature, and σ is the Stefan-Boltzmann constant (5.67×10^{-8} W m K^{-4}). If R = 0.001 m and T = 1,400 K, then P = 2.73 W

per clast. Estimates of peak radiated power from the event during e4i017tr are 1,735 GW (cosine-corrected data), 256 GW (uncorrected data), and 29 GW (uncorrected, subtracting corrected e4i006tr data). Each clast has a volume of 4.12×10^{-9} m^3 and a mass of 1.09×10^{-5} kg, assuming a density of 2,600 kg m^{-3}. Assuming we see radiation from half the clasts present, the volume of material ejected spans 89 to 5,310 m^3 (mass = 2.31×10^5 to 1.38×10^7 kg). These volumes are orders of magnitude smaller than the volumes erupted (6–13 km^3) from larger, longer duration fire fountain eruptions elsewhere on Io (Davies et al., 2001; de Pater, Davies, Adamkovics, et al., 2014).

Given the low spatial resolution of the data, it is not known with certainty if the eruption took place exactly at Marduk Fluctus, within Marduk Patera, or nearby. Rata Patera, another active volcano detected by NIMS, is located at 200°W, 36°S and may contribute to the observed radiance in the high emission angle data. Nevertheless, Marduk Fluctus seems to be the most likely candidate, based on the constancy of thermal emission as seen in these and higher spatial resolution data. Regardless of exactly where this event took place, the detection of this style of activity means that another volcanic process has been identified that designers of future Io instruments and missions need to be aware of as a suitable target for determining the eruption temperature of Io's silicate lava. Such observations would require unsaturated data of such events to be acquired simultaneously (or within ≈0.04 s; Davies et al., 2011, 2017) at multiple visible and/or infrared (≤1.5 μm) wavelengths. The chances of observing future events are good as this was a powerful eruption identified in low spatial resolution data at a great distance from Io. We are currently searching for similar hidden gems in the NIMS data set.

6. Summary

This explosive event evolved on a much faster time scale than other volcanic processes observed by NIMS and occurred on a shorter time scale and smaller areal scale than the much larger and more powerful "outburst" eruptions, characterized by fountains feeding lava flows (Davies et al., 2001). We note that the temporal resolution of the NIMS data, extraordinary as it is, leaves open the possibility that the peak of thermal emission was not seen. NIMS constrains the onset of the event to within ≈2 hr. We do not know how big this event might have been, or how rapid the waxing phase was—but we do observe that the thermal source decayed quickly (in a few minutes), consistent with an abrupt, explosive event. If correctly imaged, such an event may be appropriate for determining lava eruption temperature by instruments on spacecraft, even at hundreds of thousands of kilometers from Io.

Acknowledgments
This work was performed at the Jet Propulsion Laboratory-California Institute of Technology, under contract to NASA. We thank A.S. McEwen and D.A. Williams for their reviews. A.G.D. thanks the NASA Outer Planets Research and Planetary Geology and Geophysics Programs for past support under awards NNN13D466T and NMO710830. The research was partially supported by the National Science Foundation, NSF grant AST-1313485 to UC Berkeley. L.W. thanks the Leverhulme Trust for an Emeritus Fellowship. NIMS data are available from the NASA Planetary Data System.
© Caltech 2018.

References

Becker, T., & Geissler, P. E. (2005). *Galileo* global color mosaics of Io. 36th Lunar and Planetary Science Conference. Abstract 1862, on CD-ROM.

Belton, M. J. S., Head, J. W. I. I. I., Ingersoll, A. P., Greeley, R., McEwen, A., Klaasen, K. P., et al. (1996). *Galileo*'s first images of Jupiter and the Galilean satellites. *Science*, *274*(5286), 377–385. https://doi.org/10.1126/science.274.5286.377

Blaney, D. L., Johnson, T. V., Matson, D. L., & Veeder, G. J. (1995). Volcanic eruptions on Io: Heat flow, resurfacing, and lava composition. *Icarus*, *113*(1), 220–225. https://doi.org/10.1006/icar.1995.1020

Carlson, R. W., Weissman, P. R., Smythe, W. D., & Mahoney, J. C. (1992). Near-infrared mapping spectrometer experiment on *Galileo*. *Space Science Reviews*, *60*, 457–502.

Davies, A. G. (1996). Io's volcanism: Thermo-physical models of silicate lava compared with observations of thermal emission. *Icarus*, *124*(1), 45–61. https://doi.org/10.1006/icar.1996.0189

Davies, A. G. (2003). Volcanism on Io: Estimation of eruption parameters from *Galileo* NIMS data. *Journal of Geophysical Research*, *108*(E9), 5106. https://doi.org/10.1029/2001JE001509

Davies, A. G. (2007). *Volcanism on Io: A comparison with Earth* (p. 376). Cambridge: Cambridge University Press. https://doi.org/10.1017/CBO9781107279902

Davies, A. G., Calkins, J., Scharenbroich, L., Vaughan, R. G., Wright, R., Kyle, P., et al. (2008). Multi-instrument remote and *in-situ* observations of the Erebus volcano (Antarctica) lava lake in 2005: A comparison with the Pele lava lake on the Jovian moon Io. *Journal of Volcanology and Geothermal Research*, *177*(3), 705–724. https://doi.org/10.1016/j.jvolgeores.2008.02.010

Davies, A. G., Gunapala, S., Soibel, A., Ting, D., Rafol, S., Blackwell, M., et al. (2017). A novel technology for measuring the eruption temperature of silicate lavas with remote sensing: Application to Io and other planets. *Journal of Volcanology and Geothermal Research*, *343*, 1–16. https://doi.org/10.1016/j.jvolgeores.2017.04.016

Davies, A. G., Keszthelyi, L. P., & Harris, A. J. L. (2010). The thermal signature of volcanic eruptions on Io and Earth. *Journal of Volcanology and Geothermal Research*, *194*(4), 75–99. https://doi.org/10.1016/j.jvolgeores.2010.04.009

Davies, A. G., Keszthelyi, L., & McEwen, A. S. (2011). Estimating eruption temperature from thermal emission spectra of lava fountain activity in the Erta'Ale (Ethiopia) volcano lava lake—Implications for observing Io's volcanoes. *Geophysical Research Letters*, *38*, L21308. https://doi.org/10.1029/2011GL049418

Davies, A. G., Keszthelyi, L. P., & McEwen, A. S. (2016). Determination of eruption temperature of Io's lavas using lava tube skylights. *Icarus*, *278*, 266–278. https://doi.org/10.1016/j.icarus.2016.06.003

Davies, A. G., Keszthelyi, L. P., Williams, D. A., Phillips, C. B., McEwen, A. S., Lopes, R. M. C., et al. (2001). Thermal signature, eruption style, and eruption evolution at Pele and Pillan on Io. *Journal of Geophysical Research*, *106*(E12), 33,079–33,103. https://doi.org/10.1029/2000JE001357

Davies, A. G., McEwen, A. S., Lopes-Gautier, R., Keszthelyi, L., Carlson, R. W., & Smythe, W. D. (1997). Temperature and Area constraints of the South Volund volcano on Io from the NIMS and SSI Instruments during the Galileo G1 orbit. *Geophysical Research Letters*, *24*, 2447–2450. https://doi.org/10.1029/97GL02310

Davies, A. G., Veeder, G. J., Matson, D. L., & Johnson, T. V. (2012). Io: Charting thermal emission variability with the *Galileo* NIMS Io thermal emission database (NITED): Loki Patera. *Geophysical Research Letters*, *39*, L01201. https://doi.org/10.1029/2011GL049999

de Kleer, K., & de Pater, I. (2017). Io's Loki Patera: Modeling of three brightening events in 2013–2016. *Icarus*, *289*, 181–198. https://doi.org/10.1016/j.icarus.2017.01.038

de Pater, I., Davies, A. G., Adamkovics, M., & Ciardi, D. R. (2014). Two new, rare, high-effusion outburst eruptions at Rarog and Heno Paterae on Io. *Icarus*, *242*, 365–378. https://doi.org/10.1016/j.icarus.2014.06.016

de Pater, I., Davies, A. G., McGregor, A., Trujillo, C., Ádámkovics, M., Veeder, G. J., et al. (2014). Global near-IR maps from Gemini-N and Keck in 2010, with a special focus on Janus Patera and Kanehekili Fluctus. *Icarus*, *242*, 379–395. https://doi.org/10.1016/j.icarus.2014.06.019

Geissler, P. E., McEwen, A. S., Keszthelyi, L., Lopes-Gautier, R., Granahan, J., & Simonelli, D. P. (1999). Global color variations on Io. *Icarus*, *140*(2), 265–282. https://doi.org/10.1006/icar.1999.6128

Gerst, A., Hort, M., Aster, R. C., Johnson, J. B., & Kyle, P. R. (2013). The first second of volcanic eruptions from the Erebus volcano lava lake, Antarctica—Energies, pressures, seismology, and infrasound. *Journal of Geophysical Research: Solid Earth*, *118*, 3318–3340. https://doi.org/10.1002/jgrb.50234

Gerst, A., Hort, M., Kyle, P. R., & Vöge, M. (2008). 4D velocity of Strombolian eruptions and man-made explosions derived from multiple Doppler radar instruments. *Journal of Volcanology and Geothermal Research*, *177*(3), 648–660. https://doi.org/10.1016/j.jvolgeores.2008.05.022

Houghton, B. F., Swanson, D. A., Carey, R. J., Rausch, J., & Sutton, A. J. (2011). Pigeonholing pyroclasts: Insights from the 19 March 2008 explosive eruption of Kılauea volcano. *Geology*, *39*, 262–266.

Keszthelyi, L., Jaeger, W., Milazzo, M., Radebaugh, J., Davies, A. G., & Mitchell, K. (2007). New estimates for Io eruption temperatures: Implications for the interior. *Icarus*, *192*(2), 491–502. https://doi.org/10.1016/j.icarus.2007.07.008

Keszthelyi, L., McEwen, A. S., Phillips, C. B., Milazzo, M., Geissler, P., Turtle, E. P., et al. (2001). Imaging of volcanic activity on Jupiter's moon Io by *Galileo* during the *Galileo* Europa mission and the *Galileo* millennium mission. *Journal of Geophysical Research*, *106*(E12), 33,025–33,052. https://doi.org/10.1029/2000JE001383

Leone, G., Wilson, L., & Davies, A. G. (2011). The geothermal gradient of Io: Consequences for lithosphere structure and volcanic eruptive activity. *Icarus*, *211*(1), 623–635. https://doi.org/10.1016/j.icarus.2010.10.016

Lopes-Gautier, R., Davies, A. G., Carlson, R., Smythe, W., Kamp, L., Soderblom, L., et al. (1997). Hot spots on Io: Initial results from *Galileo*'s near infrared mapping spectrometer. *Geophysical Research Letters*, *24*(20), 2439–2442. https://doi.org/10.1029/97GL02662

Mastin, L. G. (1997). Evidence for water influx from a caldera lake during the explosive hydromagmatic eruption of 1790, Kilauea volcano, Hawai'i. *Journal of Geophysical Research*, *102*, 20,093–20,109. https://doi.org/10.1029/97JB01426

McEwen, A. S., Keszthelyi, L., Spencer, J. R., Schubert, G., Matson, D. L., Lopes-Gautier, R., et al. (1998). High-temperature silicate volcanism on Jupiter's moon Io. *Science*, *281*(5373), 87–90. https://doi.org/10.1126/science.281.5373.87

McEwen, A. S., Simonelli, D. P., Senske, D. R., Klaasen, K. P., Keszthelyi, L., Johnson, T. V., et al. (1997). High-temperature hot spots on Io as seen by the *Galileo* Solid State Imaging (SSI) experiment. *Geophysical Research Letters*, *24*(20), 2443–2446. https://doi.org/10.1029/97GL01956

Orr, T., Thelin, W. A., Patrick, M. P., Swanson, D. A., & Wilson, D. C. (2013). Explosive eruptions triggered by rockfalls at Kilauea volcano, Hawai'i. *Geology*, *41*(2), 207–210. https://doi.org/10.1130/G33564.1

Radebaugh, J., McEwen, A. S., Milazzo, M., Davies, A. G., Keszthelyi, L. P., & Geissler, P. (2002). *Galileo* SSI and *Cassini* ISS observations of Io's Pele hotspot: Temperatures, areas, and variation with time. *Lunar and Planetary Institute Conference Abstracts*, *33*, 1445.

Sinton, W. M., Lindwall, D., Cheigh, F., & Tittemore, W. C. (1983). Io—The near-infrared monitoring program, 1979–1981. *Icarus*, *54*(1), 133–157. https://doi.org/10.1016/0019-1035(83)90074-X

Strom, R. G., Schneider, N. M., Terrile, R. J., Cook, A. F., & Hansen, C. (1981). Volcanic eruptions on Io. *Journal of Geophysical Research*, *86*(A10), 8593–8620. https://doi.org/10.1029/JA086iA10p08593

Veeder, G. J., Davies, A. G., Matson, D. L., & Johnson, T. V. (2009). Dark flow fields on Io. *Icarus*, *204*(1), 239–253. https://doi.org/10.1016/j.icarus.2009.06.027

Veeder, G. J., Davies, A. G., Matson, D., Johnson, T. V., Williams, D. A., & Radebaugh, J. (2012). Io: Volcanic thermal sources and global heat flow. *Icarus*, *219*(2), 701–722. https://doi.org/10.1016/j.icarus.2012.04.004

Williams, D. A., Keszthelyi, L. P., Crown, D. A., Yff, J. A., Jaeger, W. L., Schenk, P. M., et al. (2011). Volcanism on Io: New insights from global geologic mapping. *Icarus*, *214*(1), 91–112. https://doi.org/10.1016/j.icarus.2011.05.007

Wilson, L., & Head, J. W. (1981). Ascent and eruption of basaltic magma on the Earth and Moon. *Journal of Geophysical Research*, *86*(B4), 2971–3001. https://doi.org/10.1029/JB086iB04p02971

Wilson, L., & Head, J. W. (1983). A comparison of volcanic eruption processes on Earth, Moon, Mars, Io and Venus. *Nature*, *302*(5910), 663–669. https://doi.org/10.1038/302663a0